C_{60} Molecular Bearings

K. Miura* and S. Kamiya
Department of Physics, Aichi University of Education, Hirosawa 1, Igaya -cho, Kariya 448-8542, Japan

N. Sasaki†
Department of Applied Physics, Faculty of Engineering, Seikei University, Kichijoji Kitamachi 3-3-1, Musashino-shi, Tokyo 180-8633, Japan

(Received 30 June 2002; published 7 February 2003)

An ultralubricated system is reported which confines a C_{60} monolayer between graphite plates. C_{60} molecules act as molecular bearings, assisted by the nanogears of six-membered carbon rings between C_{60} molecules and graphite, in which the mean dynamical frictional forces are zero up to a high load of 100 nanonewtons. A stick-slip rolling model with a step rotation of a C_{60} molecule is proposed. This ultralubricated system, very promising for the realization of nano- and micromachines, is expected to open a new field of molecular bearings.

DOI: 10.1103/PhysRevLett.90.055509 PACS numbers: 61.48.+c, 81.40.Pq

Nano- and micromachines have been expected to trigger the creation of a future prominent industry. As first suggested by Feynman [1], molecular bearings have been expected to be a fundamental component of many molecular mechanical devices performing a frictionless system and to be very effective for the realization of nano- and micromachines. However, previous work on micromachine bearings has produced poor results, both experimentally and theoretically. Thus far, micromachines have been considered "machines incapable of movement." At this time, it has been expected that fullerenes would be the ultimate lubricant; however, unfortunately, it has been found that the addition of C_{60} between two surfaces is of little use. On the other hand, it has been reported that intercalation of C_{60} into graphite caused the material to act as a fluid under load [2]. In this Letter, we focus on C_{60} molecular bearings. In previous papers [3–6], it has been reported that C_{60} molecules on graphite can grow in monolayer form, which consists of close-packed C_{60} molecules. Thus, the C_{60} molecules form a commensurate monolayer on graphite. Experimentally, this finding has been clarified by Okita and Miura [5]. Theoretically, it has been also clarified by Gravil *et al.* [3] that a C_{60} molecule forms *AB* stacking with graphite. Since the six-membered ring of a C_{60} molecule stacks on that of graphite such that the *AB* stacking of graphite is maintained, a graphite flake placed on the C_{60} monolayer on graphite is expected to stack in the same way as the C_{60} molecules on graphite. Thus, we can construct a system confining a C_{60} monolayer between graphite plates, which forms the nanogears of six-membered rings between C_{60} molecules and graphite.

A graphite substrate was prepared by cleaving highly oriented pyrolytic graphite (HOPG). The C_{60} films on HOPG were prepared by evaporation from a boron nitride crucible. The substrate temperatures during evaporation were kept in the range of 150 to 200 °C. A cleavaged graphite flake with an area of 1 mm square and a thickness of several micrometers was used. Coordinate data of C_{60} films on graphite (C_{60} films/graphite) were stored as memory data on a computer because the C_{60} films/graphite base is fixed with respect to a tip position. That is to say, in our experimental setup, whether the graphite flake is set on the C_{60} films/graphite or not gives no influences on the determination of a tip position. The tip position is directly determined by the previously obtained data of C_{60} films/graphite. Hence, a manipulator was used to put a graphite flake on a suitable location of the fixed C_{60} films/graphite, and, thereafter, a rectangular silicon cantilever with normal spring constants of 0.75 N/m was placed on the graphite flake on the C_{60} films/graphite by using the coordinate data of C_{60} films/graphite within an experimental error of submicrometer [7]. Normal and lateral forces were measured simultaneously under humidity-controlled conditions at room temperature using a commercially available instrument (Seiko Instruments Inc., SPI-3700). The scan speed was 0.13 μm/s. Zero normal force was defined as the position at which the cantilever was not bent. The frictional forces were calibrated by using the method presented in previous papers [4–6].

Shown in Fig. 1 are topographs (atomic force microscope images) of graphite (area S_A), C_{60} monolayers on graphite (area S_B), and C_{60} bilayers on graphite (area S_C). When a graphite flake is placed on areas S_A, S_B, and S_C, the graphite flake on graphite (*D*), the graphite flake on the C_{60} monolayer/graphite (which we call graphite/C_{60}^{mono}/graphite: *E*), and the graphite flake on the C_{60} bilayer/graphite (graphite/C_{60}^{bilayer}/graphite: *F*) are obtained, respectively. As shown in Fig. 1, frictional force maps for graphite (*A*) show that the tip exhibits one-dimensional stick-slip and two-dimensional zigzag stick-slip motions for $[12\bar{3}0]$ and $[10\bar{1}0]$ scanning directions, respectively [8,9], although they exhibit significant load dependence at small loads [8,9]. Frictional force maps for *B* and *C* show that the tip exhibits one-dimensional

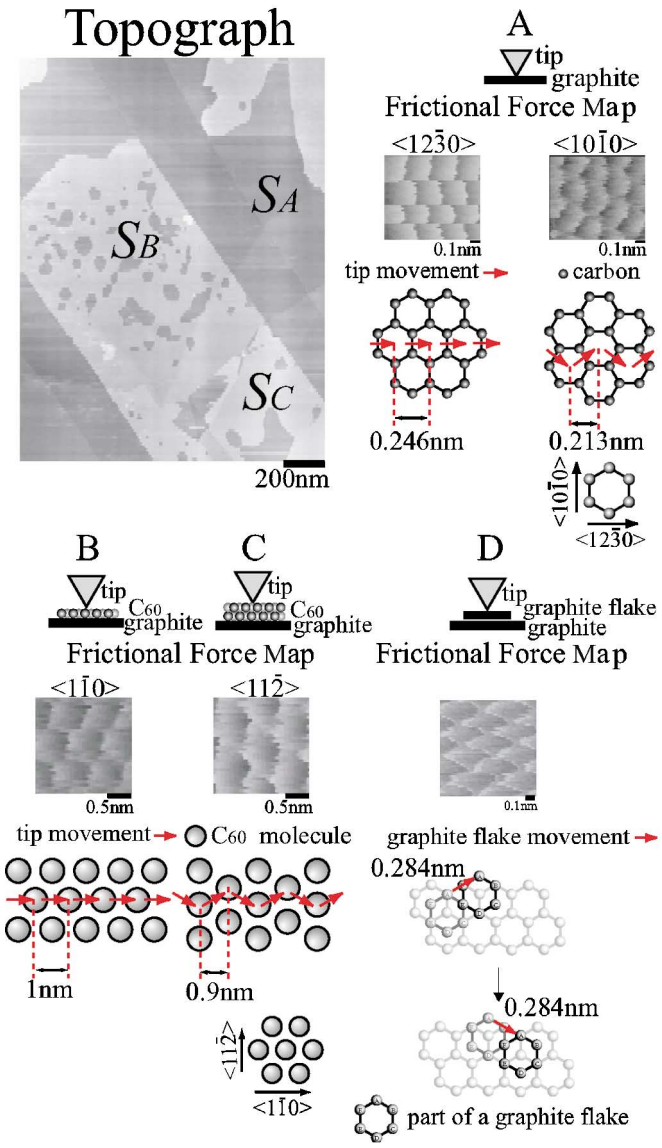

FIG. 1 (color). Topographs (atomic force microscope images) for graphite (area S_A), C_{60} monolayers on graphite (area S_B), and C_{60} bilayers on graphite (area S_C). Frictional force maps and tip movements for representative scan directions for graphite (*A*), C_{60} monolayers on graphite (*B*), amd C_{60} bilayers on graphite (*C*). A frictional force map and a flake movement for graphite flake on graphite (*D*). Frictional force maps and tip movements for (*B*) and (*C*) are the same.

stick-slip and two-dimensional stick-slip motions for the [1$\bar{1}$0] and [11$\bar{2}$] scanning directions of a C_{60}(111) surface, respectively [4,5]; it is more difficult to obtain clear frictional force maps for a C_{60} monolayer than for a C_{60} bilayer because the C_{60} monolayer is unstable for a tip contact. The frictional force maps for *B* show that the C_{60} monolayer consists of close-packed C_{60} molecules. This indicates that a six-membered ring is stacked on the graphite such that the *AB* stacking of graphite is maintained, and thus the six-membered ring is situated at the top of C_{60} molecules [5,6]. The frictional force map for *D* shows that the graphite flake moves on the graphite such that the *AB* stacking of graphite is maintained [9]. Assuming that the graphite flake stacks on C_{60} molecules in the same way as C_{60} molecules stack on graphite, the projection of the first-layer six-membered net of the graphite flake is expected to be completely coincident with that of the graphite substrate through a C_{60} monolayer.

Figure 2 shows frictional force maps versus loading force for the graphite/C_{60}^{mono}/graphite (*E*). It should be noted that the maps of *E* show transient patterns in relation to loading force, clearly different from those for graphite (*A*) [8,9], C_{60}(111) surfaces [4,5] (*B* and *C*) and the graphite flake on graphite (*D*) [9] from the standpoint of periodic pattern and contrast, as shown in Fig. 1. Noting that this system includes friction between a tip and a graphite flake and that between a C_{60} monolayer and two graphite plates, it is considered that the friction from this system involves two different frictional mechanisms.

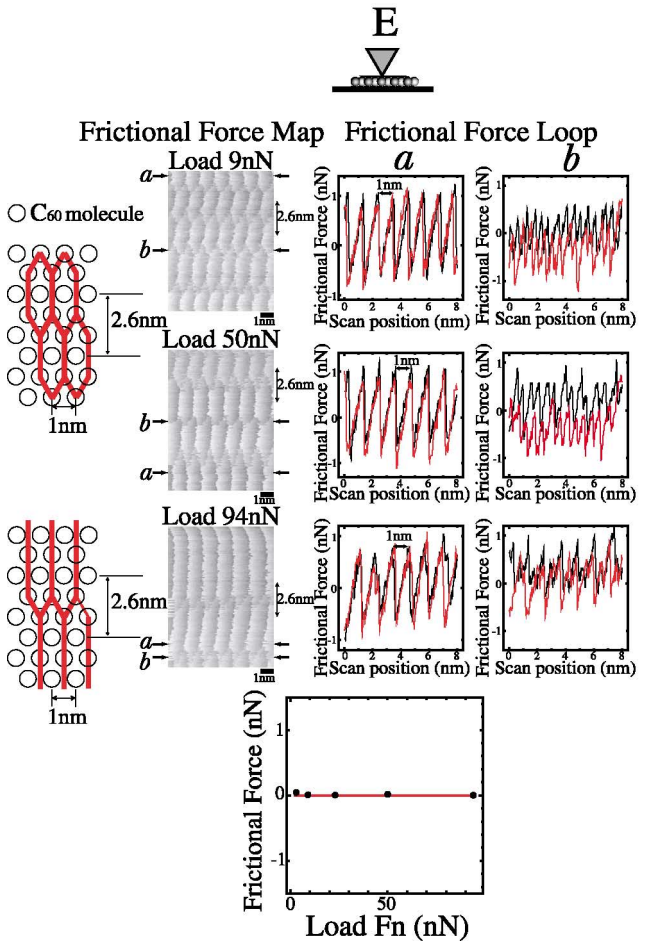

FIG. 2 (color). Frictional force maps versus loading force for graphite/C_{60}^{mono}/graphite (*E*). Frictional force loops obtained from line profiles shown by arrows *a* and *b* in the frictional force maps are also represented, where the black and red lines indicate one direction and in the opposite direction, respectively. Supercell structures of the frictional force maps are illustrated on the left-hand side. Mean frictional forces versus loading force shown by arrow *a* is shown on the bottom.

However, it is reasonable that the frictional features of this system show only friction between the C_{60} monolayer and the two graphite plates because they do not show a frictional force map like that obtained for graphite (A) at all. This leads to the conclusion that the friction between the tip and the graphite flake is greater than that between the C_{60} monolayer and two graphite plates. Thus, the graphite flake moves together with the tip during scanning. At this point we note that the frictional force map at a load of 9 nN has a periodicity of 1 nm along the x direction and a periodicity of 2.6 nm along the y direction. This reflects the close-packed C_{60} molecular arrangement, as shown in Fig. 2, but has a supercell structure (a periodicity of 2.6 nm) along the y direction. Furthermore, these maps exhibit a vertical chainlike transient pattern related to loading force. It should be noted that the frictional loops obtained from line profiles shown by arrow a in the frictional force maps do not exhibit hysteresis in both directions, which indicates that the mean frictional forces are zero and thus there is no energy dissipation [10], although those shown by arrow b accompany some hysteresis, in which two-dimensional zigzag motions of a graphite flake exhibit. As shown on the bottom of Fig. 2, the mean frictional forces at position a are zero up to a high load, although the frictional forces have a finite value. Then, the maximum frictional force in this experiment is estimated to be below 1 nN, which is comparable to the shear force (0.4 nN) between a C_{60} single molecule and graphite [5].

If the nanogears of six-membered rings between C_{60} molecules and the upper and lower graphite plates are formed in this system, it is found to be easy to apply torque to C_{60} molecules via their gears as shown in Fig. 3(a). Thus, it is possible that C_{60} molecules roll by means of torque, which is estimated to be approximately 1.0×10^{-19} N m. This indicates that the rolling of C_{60} molecules occurs easily along the $[12\bar{3}0]$ direction using one side of a six-membered ring. However, there exist only four six-membered rings along a great circle of a C_{60} molecule, which does not always mean that the six-membered ring situates on the top of the C_{60} molecule after rolling. Now, the energetic barrier for rotation of a C_{60} molecule around the [0001] axis of a graphite substrate is estimated to be a few meV by Gravil *et al.* [3]. Therefore it is possible that the discrete step rotations of a C_{60} molecule between the positions holding AB stacking around this axis are induced by thermal excitations at room temperature. This step rotation allows C_{60} molecules to roll so that a low-friction force generates. For example, when the rotation around the [0001] axis occurs, the rolling of the C_{60} molecule with the step rotation at the six-membered ring 1 occurs equivalently toward rings 2, 3, and 4. Assuming that the C_{60} molecule rolls toward ring 2, the next rolling occurs equivalently toward rings 1, 5, and 6. Assuming that the C_{60} molecule rolls toward ring 5, the six-membered ring of the C_{60} molecule facing the graphite surface advances such as $1 \rightarrow 2 \rightarrow 5$ as

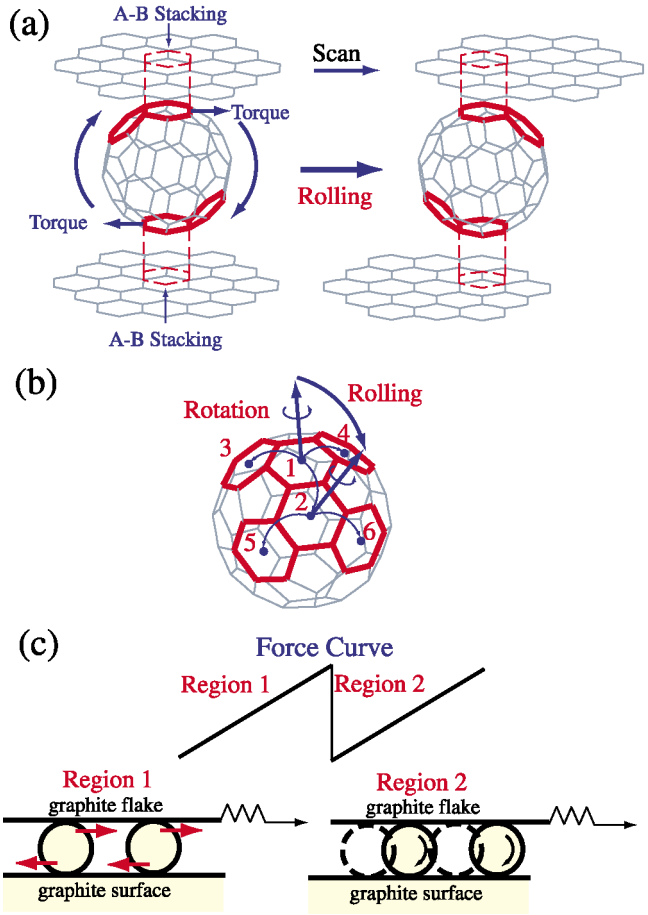

FIG. 3 (color). The stick-slip rolling model with a step rotation of a C_{60} molecule. (a) C_{60} molecules roll by means of torque, which is produced by the nanogears of six-membered rings between C_{60} molecules and the upper and lower graphite plates. (b) The discrete step rotation of a C_{60} molecule around the [0001] axis is illustrated. (c) In region 1, C_{60} molecules stick but thermal rotations around the [0001] axis occur. In region 2, C_{60} molecules slip in both rolling and translational motions (bottom figure).

shown in Fig. 3(b). Thus, a stick-slip process for rolling and translational motions is given as follows. In region 1 in Fig. 3(c), C_{60} molecules stick but thermal rotations around the [0001] axis occur. In region 2 in Fig. 3(c), C_{60} molecules slip in both rolling and translational motions. Then, nearly all the potential energies stored by a cantilever transform into rolling and translational motions. Thus, it should be noted that friction heat does not generate in this system. At present, a total energy calculation with a rigid model is performed, but it does not reproduce the frictional force maps with a supercell structure [11]. Furthermore, it is an open question whether the coherent rolling of C_{60} molecules occurs or not because the contact area between a graphite flake and a C_{60} monolayer is unclear. It can be expected that the van der Waals interaction between C_{60} molecules significantly influences the collective motion of C_{60} molecules, which can produce the supercell structure in frictional force maps.

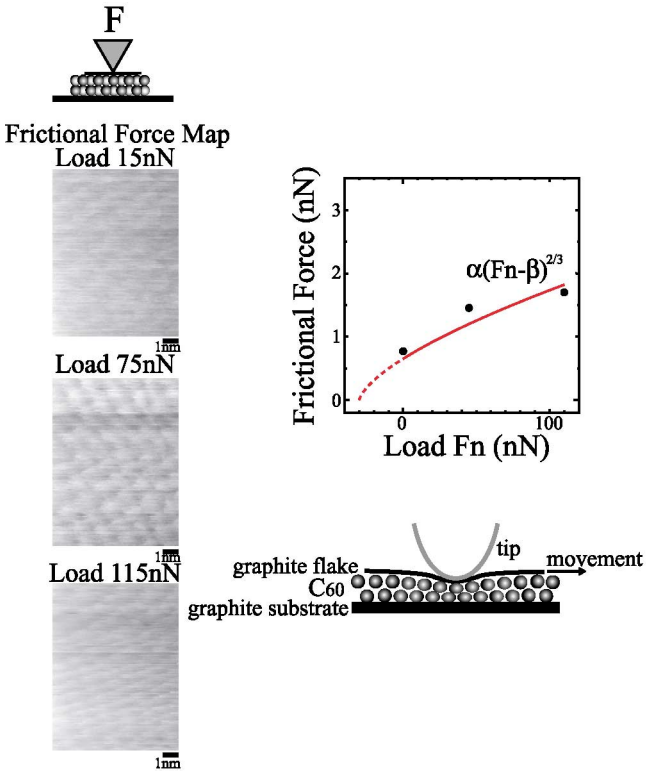

FIG. 4 (color). The frictional force maps and the curve of mean frictional force versus loading force for graphite/$C_{60}^{bilayer}$/graphite (*F*). The frictional force maps for graphite/$C_{60}^{bilayer}$/graphite (*F*) do not exhibit clear load dependence although they feature periodic patterns. The curve of mean frictional force versus loading force from graphite/$C_{60}^{bilayer}$/graphite behaves in the same manner as does the Herztian contact, because the solid line is defined as $\alpha(F_n^{2/3} - \beta)$ in relation to the loading force F_n with α and β estimated to be 0.068 and 30 nN, respectively.

Hence, molecular dynamical calculations considering rolling, rotation, and translation of C_{60} molecules and deformations of graphite and C_{60} molecules are now being performed.

The appearance of the vertical chainlike pattern with larger loads indicates the increase of the deformations of C_{60} molecules which leads to the vertical chainlike pattern by decreasing C_{60} nearest-neighbor distances. Here, it may be interesting to note that the deformations of the C_{60} monolayer induce a transition from a semiconductor phase to a metal phase [12].

As shown in Fig. 4, the frictional force maps for graphite/$C_{60}^{bilayer}$/graphite (*F*) are also clearly different from those for graphite (*A*) [8,9], C_{60}(111) surfaces (*B* and *C*) [4,5], the graphite flake on graphite (*D*) [9], and graphite/C_{60}^{mono}/graphite (*E*) from the standpoint of periodic pattern and contrast, as shown in Figs. 1 and 2. The frictional force maps for graphite/$C_{60}^{bilayer}$/graphite (*F*) do not exhibit clear load dependence although they feature periodic patterns. As shown on the bottom of Fig. 4, plots of mean frictional force versus loading force for graphite/$C_{60}^{bilayer}$/graphite (*F*) are shown. The curve of frictional force versus loading force from graphite/$C_{60}^{bilayer}$/graphite behaves in the same manner as does the Herztian contact, because the solid line is defined as $\alpha(F_n^{2/3} - \beta)$ in relation to the loading force F_n with α and β estimated to be 0.068 and 30 nN, respectively. Thus, this indicates that the C_{60} bilayer confined by graphite plates behaves as an elastic body. Furthermore, it should be noted that as C_{60} molecular layers become thick, the frictional force maps from *E* and *F* disappear but the frictional force map from graphite is reproduced. This indicates that the tip executes stick-slip motions on the graphite flake so that the C_{60} molecules and graphite substrate situated below the graphite flake do not move as well as the graphite flake because the combined shear force between the C_{60} layers and the shear force between the C_{60} molecules and graphite plate become larger than the shear force between the tip and the graphite flake.

In this Letter, the applicability and realization of C_{60} molecular bearings is reported for the first time and the detailed mechanism of their movement is discussed. A rolling stick-slip model with a step rotation of a C_{60} molecule is proposed. The novel frictional mechanism is realized in the graphite/C_{60}^{mono}/graphite system, in which static frictional forces have a finite value but mean dynamical frictional forces are zero. It should be noted that an extremely low-friction motion can be realized only in the system which confines a C_{60} monolayer between graphite plates, where the nanogears of six-membered carbon rings between C_{60} molecules and graphite play an important role.

We thank Y. Higashijima, M. Ojima, and Y. Kumazawa for experimental assistance. This work was partially supported by "Organization and Function," PRESTO, JST.

*To whom correspondence should be addressed.
Electronic address: kmiura@auecc.aichi-edu.ac.jp
†Permanent address: Precursory Research for Embryonic Science and Technology (PRESTO), Japan Science and Technology Corporation (JST), 4-1-8 Honcho, Kawaguchi-shi, Saitama 332-0012, Japan.

[1] R. Feynman, Eng. Sci. **23**, 22 (1960).
[2] B. A. Averill *et al.*, Mol. Cryst. Liq. Cryst. **244**, 77 (1994).
[3] P. A. Gravil *et al.*, Phys. Rev. B **53**, 1622 (1996).
[4] S. Okita, M. Ishikawa, and K. Miura, Surf. Sci. **442**, L959 (1999).
[5] S. Okita and K. Miura, Nano Lett. **1**, 101 (2001).
[6] K. Miura, T. Takagi, S. Kamiya, T. Sahashi, and M. Yamauchi, Nano Lett. **1**, 161 (2001).
[7] K. Miura and S. Kamiya, Europhys. Lett. **58**, 610 (2002).
[8] N. Sasaki, K. Kobayashi, and M. Tsukada, Phys. Rev. B **54**, 2138 (1996).
[9] K. Miura, S. Kamiya, and N. Sasaki (unpublished).
[10] The hysteresis of the piezoactuator is extremely small within a nanometer scan.
[11] N. Sasaki (to be published).
[12] J. Nakamura, T. Nakayama, S. Watanabe, and M. Aono, Phys. Rev. Lett. **87**, 48301 (2001).